Ionics (2013) 19:1843–1848
DOI 10.1007/s11581-013-0918-x

ORIGINAL PAPER

Surface nitridation induced high electrochemical performance of $Li_4Ti_5O_{12}$ using urea as a nitrogen source

Xiaomei Zhao · Qun Zhou · Hai Ming · Jason Adkins · Mangmang Liu · Lele Su · Junwei Zheng

Received: 11 April 2013 / Accepted: 7 May 2013 / Published online: 22 May 2013

Abstract Surface nitridation of the $Li_4Ti_5O_{12}$ particles was carried out by thermal treatment with urea as the nitrogen source in a controllable manner. The titanium nitride (TiN) was formed in the well-dispersed zones on the surface of the $Li_4Ti_5O_{12}$ particles, depending on the coverage of the nitride. The surface TiN formed led to a great improvement of the conductivity of the oxide. The extent of the surface nitridation exhibited a large effect on electrochemical behaviors of the $Li_4Ti_5O_{12}$ particles, with the $Li_4Ti_5O_{12}$/TiN composite (prepared using 6 % urea) providing the best initial capacity and rate capability. Thus, the electrochemical performance of the $Li_4Ti_5O_{12}$ particles can be achieved by optimizing surface nitridation of the oxide. The chemically inert TiN occupied the surface sites of the $Li_4Ti_5O_{12}$ particles which may have prevented the electrolyte from decomposition and stabilized the surface structure of the $Li_4Ti_5O_{12}$ particles, endowing the oxide with excellent cycleability

Keywords Surface nitridation · Titanium nitride · Lithium titanate · Conductivity · Li-ion battery

Introduction

Li-ion batteries have proven to be an attractive power source for portable electric devices, electric vehicles, hybrid electric vehicles, and power storage devices because of their high energy density [1–3]. The commonly used anode electrode materials for the conventional lithium-ion batteries are carbon-based materials [4–7]. Such negative electrodes have low lithium-ion insertion potentials close to that of lithium metal plating [8]. This low insertion potential may induce an increased risk of internal short circuit caused by lithium metal deposition upon a rapid charge and also a risk of ignition caused by internal short circuit. For this reason, alternative anode materials are desirable for the lithium-ion batteries with high safety and long life. Spinel lithium titanate, represented by the formula $Li_4Ti_5O_{12}$ with a theoretical capacity of 175 mAh/g, has been considered to be one of the most prospective anode materials [9–11]. The oxide has excellent lithium insertion–extraction reversibility and cycleability due to a low volume change during the charge and discharge processes. The high lithium-ion insertion potential (1.55 V vs. Li^+/Li) allows $Li_4Ti_5O_{12}$, in particular, to effectively avoid the electrodeposition of the metallic lithium and decomposition of most electrolyte solvents during the charge–discharge cycling. However, $Li_4Ti_5O_{12}$ suffers from the problem of poor capacity at high rate mainly due to its low electronic conductivity. Many efforts have been devoted to overcome this problem, including synthesis of nanocrystals [12–16], cation doping [17–19], and carbon coating [20–23]. The beneficial effect of doping elements has been attributed mainly to the enhancement of the lithium diffusion. The carbon coating seems to be a successful approach to increase the electrical conductivity of the metal oxide, though a carbon coating layer may lead to a decrease in the tap density of the material. Nevertheless, a more efficient and practical way to improve the conductivity of $Li_4Ti_5O_{12}$ is still one of the main challenges in material science and manufacturing for a further enhancement of the performance of corresponding Li-ion batteries.

Recently, a very effective approach to improve the conductivity of $Li_4Ti_5O_{12}$ has been developed by introducing highly conductive titanium nitride (TiN) to the surface of the

X. Zhao · Q. Zhou · H. Ming · J. Adkins · L. Su · J. Zheng
Institute of Chemical Power Sources, Soochow University, Suzhou 215006, People's Republic of China

X. Zhao · Q. Zhou · H. Ming · M. Liu · J. Zheng (✉)
College of Chemistry, Chemical Engineering and Materials Science, Soochow University, Suzhou 215123, People's Republic of China
e-mail: jwzheng@suda.edu.cn

$Li_4Ti_5O_{12}$ particles through atomic layer deposition or annealing the material in a NH_3 atmosphere [24, 25]. The surface TiN conductive layer leads to a significant enhancement in the battery performances. However, costly reagents or processes are required by those methods. Herein, we demonstrate a facile approach to efficiently enhance the conductivity of the $Li_4Ti_5O_{12}$ powder by direct surface nitridation using urea as a soft nitridation reagent. The surface nitridation of the oxide can be easily controlled and optimized. The presence of the metallic conductive nitrides on the surface of the oxides leads to a great improvement in the rate capability and cycleability of the material.

Experimental

Sample preparation

The $Li_4Ti_5O_{12}$ powder was prepared by a modified solid-state reaction. The stoichiometric amounts of Li_2CO_3 and anatase TiO_2 with a Li/Ti molar ratio of 4:5 were mixed by planetary ball milling with acetone medium for 3 h. The mixture was calcined in a muffle furnace at 800 °C for 0.5 h to obtain white $Li_4Ti_5O_{12}$ powder. The surface nitridation of the $Li_4Ti_5O_{12}$ particles was carried out using urea as a nitridation reagent. Briefly, the $Li_4Ti_5O_{12}$ powder was mixed with different amount of urea by planetary ball milling. The mixture was calcined in a tube furnace with argon flow at 800 °C for 0.5 h. The product was naturally cooled to room temperature before being exposed to air.

Characterization

The X-ray diffraction (XRD) patterns of the samples were measured on a PANalytical B.V X-ray powder diffractometer with a monochromatic Cu $K\alpha$ (λ=0.154056 nm) radiation source. The morphologies of the samples were examined on a Hitachi S-4700 scanning electron microscope and a TecnaiG2 transmission electron microscope (TEM). The Raman spectra were obtained on a Jobin Yvon HR-800 Raman spectrometer with a 633-nm Ar^+ laser.

Electrochemical measurement

The electrochemical performance of the samples was tested using coin-type CR2016 cells. The cathode electrodes were prepared according to the following procedure. The $Li_4Ti_5O_{12}$ powder was homogeneously mixed with Super P and PVDF binder in the weight ratio of 8:1:1 in *N*-methyl pyrrolidinone (NMP) to form slurry. The slurry was spread on aluminum foil using a scalpel and dried in a vacuum oven at 120 °C for 12 h to remove the NMP. After drying, the aluminum foil was roll-pressed and punched out as a disk and further dried in a vacuum at 120 °C for 12 h. The electrolyte was 1.0 M $LiPF_6$ in a 1:1 (*v*/*v*) mixture of diethyl carbonate and ethylene carbonate. Celgard 2400 was used as the separator and a metallic lithium film was used as the anode electrode. The cells were assembled in a glove box filled with high purity argon gas. The electrochemical performances of the cells were measured on an Arbin automatic cycling data recording system (BT-2000) at room temperature.

Results and discussion

Component and morphology analysis of $Li_4Ti_5O_{12}$/TiN composites

Titanium oxides can be thermally transformed into pure metal nitrides in the presence of urea as the nitrogen source [26, 27]. In this case, the extent of the nitridation was carefully regulated by the relative amount of urea under the controlled experimental conditions, ensuring the nitridation reaction to occur only on the surface region of the oxides. The typical XRD patterns of the pristine $Li_4Ti_5O_{12}$ particles and $Li_4Ti_5O_{12}$/TiN composites are shown in Fig. 1(a)–(d). All of the reflections can be indexed in the Fd3m space group of the $Li_4Ti_5O_{12}$ cubic spinel structure with unit cell parameters of $a=b=c=8.358$ Å, $\beta=90°$ [28, 29]. The similarity between the XRD patterns of the $Li_4Ti_5O_{12}$/TiN composites and pristine $Li_4Ti_5O_{12}$ clearly demonstrates that structure of the bulk $Li_4Ti_5O_{12}$ was well preserved during nitridation treatment. The fact that no characteristic peaks of TiN could be detected for the $Li_4Ti_5O_{12}$/TiN composites may indicate that only a thin

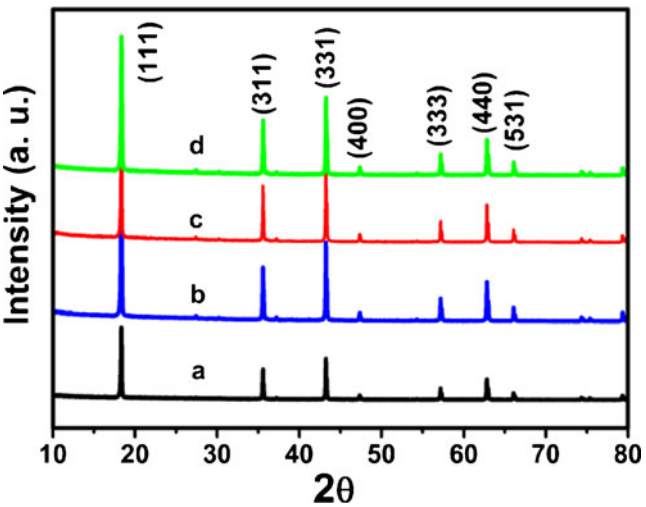

Fig. 1 XRD patterns of (*a*) pristine $Li_4Ti_5O_{12}$ and $Li_4Ti_5O_{12}$/TiN composites: (*b*) $Li_4Ti_5O_{12}$/TiN(3 %), (*c*) $Li_4Ti_5O_{12}$/TiN(6 %), and (*d*) $Li_4Ti_5O_{12}$/TiN(12 %)

layer or small amount of TiN was formed on the surface of the oxide.

Direct evidence of the formation of TiN comes from the Raman measurements, the results are shown in Fig. 2. The spectrum of the pristine $Li_4Ti_5O_{12}$ is dominated by three main bands located at 232, 428, and 670 cm^{-1}, corresponding to the F_{2g}, E_g, and A_{1g} modes, respectively [30, 31]. The surface nitridation results in appearance of the characteristic band of TiN at 152 cm^{-1}, which has been assigned to the first-order transverse acoustic mode [32, 33]. The rest modes of TiN, such as longitudinal acoustic mode, second-order acoustic mode, and transverse optical mode, overlap with the bands of $Li_4Ti_5O_{12}$ and are not distinguishable. Furthermore, an increase in the intensity of the TiN band with increasing of the extent of the surface nitridation is also indicative of the presence of TiN on the surface of the oxide.

Figure 3 depicts the TEM images of the pristine $Li_4Ti_5O_{12}$ particles and the $Li_4Ti_5O_{12}$/TiN composites. The pristine $Li_4Ti_5O_{12}$ shows a well-defined cubic crystalline structure (Fig. 3a). As the $Li_4Ti_5O_{12}$ particles were treated with 6 % urea ($Li_4Ti_5O_{12}$/TiN(6 %)), a ca. 5-nm layer of TiN with a crystal structure (different from that of $Li_4Ti_5O_{12}$) was formed on the surface (Fig. 3b). A careful inspection of the magnified TEM image (Fig. 3c) indicates that the surface of the $Li_4Ti_5O_{12}$ particles was partially occupied by the well-dispersed TiN zones, i.e., the surface nitridation was somehow localized. Meanwhile, the HRTEM of pristine $Li_4Ti_5O_{12}$ particle displayed only one diffraction fringe with the lattice distance of 0.485 nm, matched pretty well with the fringe distance of (111) diffraction plane for spinel $Li_4Ti_5O_{12}$, and the distance of the lattice distance increased with the amount of the urea added. The coverage of TiN on the $Li_4Ti_5O_{12}$ particles strongly depends on the extent of the surface nitridation. With increased amounts of urea up to 12 % ($Li_4Ti_5O_{12}$/TiN(12 %)), the cubic structure of the $Li_4Ti_5O_{12}$ particles completely disappears (Fig. 2(d)), suggesting that the Ti atoms at surface of the $Li_4Ti_5O_{12}$ particles were completely converted into TiN.

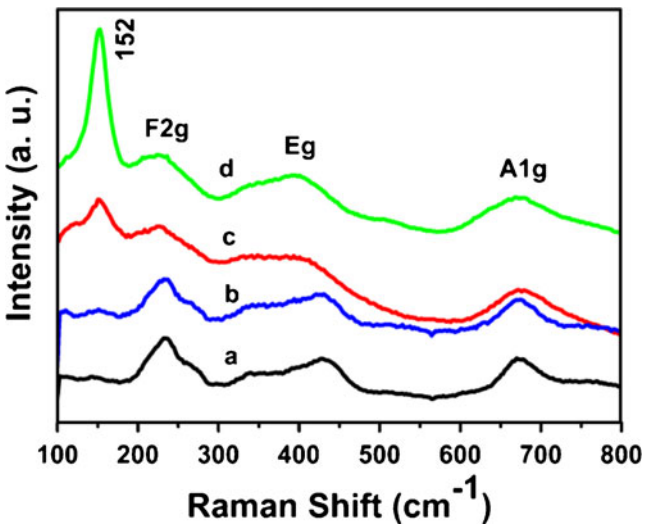

Fig. 2 Raman spectra of (*a*) pristine $Li_4Ti_5O_{12}$ and $Li_4Ti_5O_{12}$/TiN composites: (*b*) $Li_4Ti_5O_{12}$/TiN(3 %), (*c*) $Li_4Ti_5O_{12}$/TiN(6 %), and (*d*) $Li_4Ti_5O_{12}$/TiN(12 %)

Electrochemical performance of $Li_4Ti_5O_{12}$/TiN composites

The charge/discharge curves of the pristine $Li_4Ti_5O_{12}$ and $Li_4Ti_5O_{12}$/TiN composites measured at a 0.2 C rate between 0.8 and 2.5 V versus Li^+/Li are shown in Fig. 4. All the samples exhibited extremely flat charge/discharge plateaus at the voltage of about 1.55 V vs. Li^+/Li, representing the coexistence of Li 8a domains (Li occupies tetrahedral sites) with Li 16c domains (Li occupies octahedral sites) [28, 34]. The surface nitridation resulted in an increase in the initial discharge capacity of the $Li_4Ti_5O_{12}$ particles even at a relatively low rate of 0.2 C. The pristine $Li_4Ti_5O_{12}$ delivered an initial capacity of 149.4 mAh/g. For the samples with surface nitridation, the initial capacities were 168.3 mAh/g for $Li_4Ti_5O_{12}$/TiN(3 %), 170.4 mAh/g for $Li_4Ti_5O_{12}$/TiN(6 %), and 166.4 mAh/g for $Li_4Ti_5O_{12}$/TiN(12 %), respectively, which are close to the theoretical capacity of $Li_4Ti_5O_{12}$. In addition, the potential difference between the charge and discharge plateaus for the $Li_4Ti_5O_{12}$/TiN composites is much smaller than that for the pristine $Li_4Ti_5O_{12}$. This is perhaps due to the better conductivity of the $Li_4Ti_5O_{12}$/TiN composites. The higher conductivity results in less polarization of the electrode.

The improved conductivity of the $Li_4Ti_5O_{12}$/TiN composites is further confirmed by the electrochemical impedance measurements of the electrode materials, with the results shown in Fig. 5. The impedance curves of all the samples are comprised of a depressed semicircle in high- to medium-frequency range and a spike in the low-frequency range. The electrochemical reaction resistances, estimated from the semicircles in the impedance curves, are 17.5 Ω/cm^2 for pristine $Li_4Ti_5O_{12}$, 8.5 Ω/cm^2 for $Li_4Ti_5O_{12}$/TiN(3 %), 7 Ω/cm^2 for $Li_4Ti_5O_{12}$/TiN(6 %), and 5 Ω/cm^2 for $Li_4Ti_5O_{12}$/TiN(12 %). It is evident that the formation of the surface TiN largely improves electrical performance of the $Li_4Ti_5O_{12}$ particles.

Rate capacity and cycleability of $Li_4Ti_5O_{12}$/TiN composites

The rate capability behaviors of the samples charged and discharged at the same C rates up to maximum 10 C are shown in Fig. 6. At very low rate (0.1 C), the surface TiN showed only a slight effect on the capacity of the $Li_4Ti_5O_{12}$ particles. At a higher C rate, however, the $Li_4Ti_5O_{12}$/TiN composites exhibited superior rate capacity performance, relative to the pristine $Li_4Ti_5O_{12}$. In particular, the $Li_4Ti_5O_{12}$/TiN(6 %) composite exhibited the best

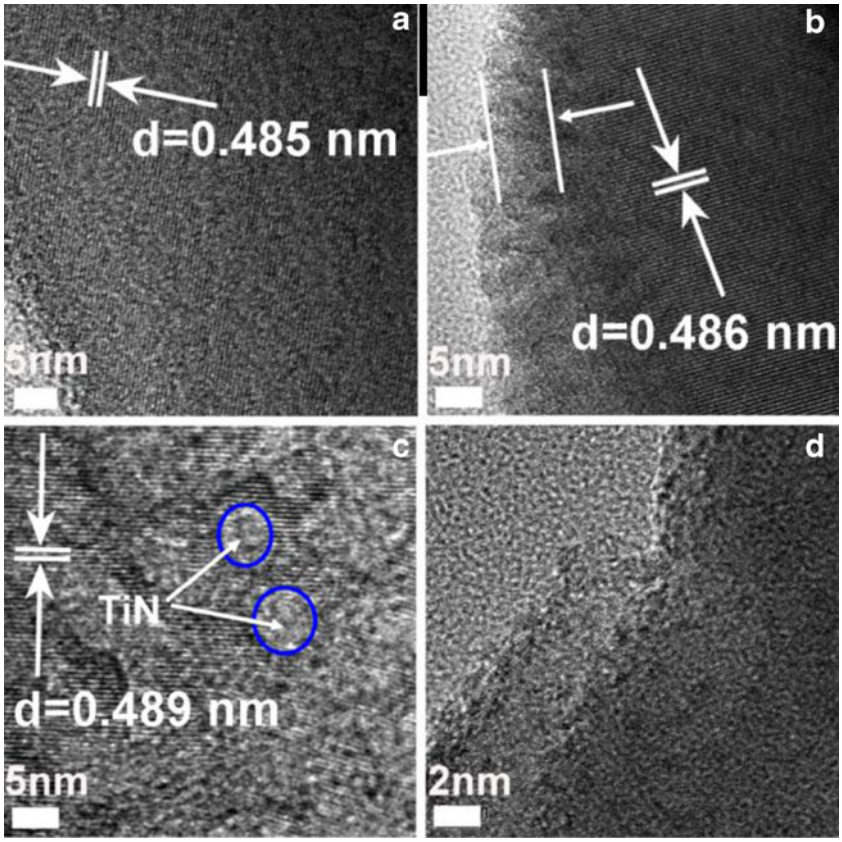

Fig. 3 HRTEM graphs of **a** pristine $Li_4Ti_5O_{12}$; **b** $Li_4Ti_5O_{12}$/TiN(6 %); **c** $Li_4Ti_5O_{12}$/TiN (6 %) (magnified); and **d** $Li_4Ti_5O_{12}$/TiN(12 %)

electrochemical performance with a specific capacity of 116.1 mAh/g at 10 C rate. The pristine $Li_4Ti_5O_{12}$ can only deliver a very low capacity (66.5 mAh/g) at the same rate. On the other hand, for all the samples, less than 1 % capacity was lost after changing the current density from 0.1 to 10 C and back to 0.1 C in 40 cycles, showing a good stability of both the pristine $Li_4Ti_5O_{12}$ and $Li_4Ti_5O_{12}$/TiN composites. It is noteworthy that a difference in the rate capacities between the $Li_4Ti_5O_{12}$/TiN composites was also observed. For example, the specific capacities for the $Li_4Ti_5O_{12}$/TiN(3 %), $Li_4Ti_5O_{12}$/TiN(6 %), and $Li_4Ti_5O_{12}$/TiN(12 %) composites were 129.7, 145.2, and 126.1 mAh/g, respectively, at 5 C rate. The $Li_4Ti_5O_{12}$/TiN(6 %) composite delivered the highest capacity. This implies that the extent of the surface

Electrochemical performance of $Li_4Ti_5O_{12}$/TiN composites

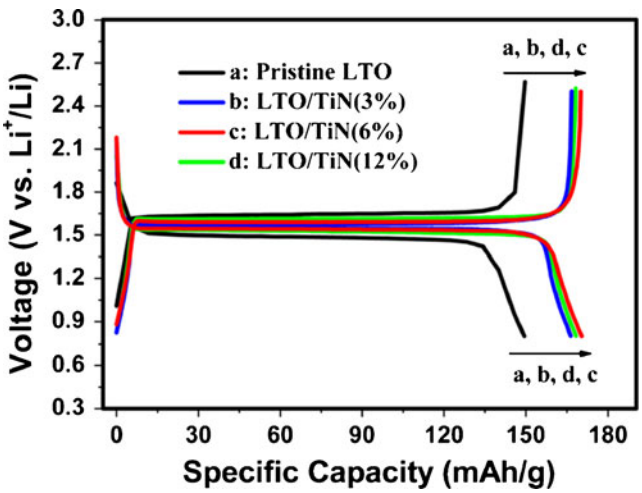

Fig. 4 Charge/discharge curves of pristine $Li_4Ti_5O_{12}$ and $Li_4Ti_5O_{12}$/TiN composites at discharge rate of 0.2 C

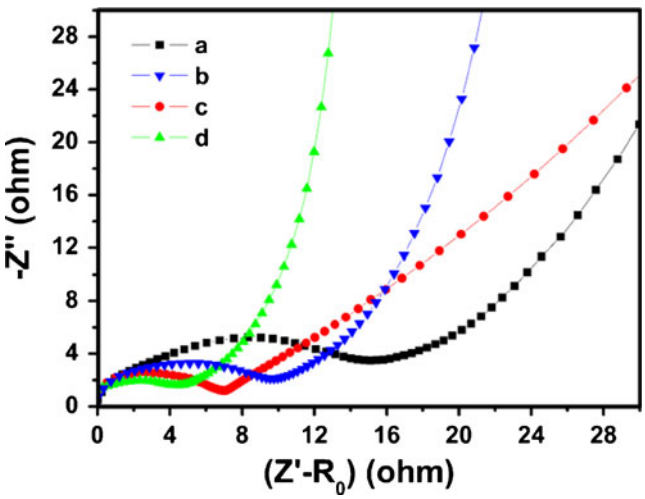

Fig. 5 Electrochemical impedance spectra of (*a*) pristine $Li_4Ti_5O_{12}$ and $Li_4Ti_5O_{12}$/TiN composites: (*b*) $Li_4Ti_5O_{12}$/TiN(3 %), (*c*) $Li_4Ti_5O_{12}$/TiN(6 %), and (*d*) $Li_4Ti_5O_{12}$/TiN(12 %)

Rate capacity and cycleability of $Li_4Ti_5O_{12}$/TiN composites

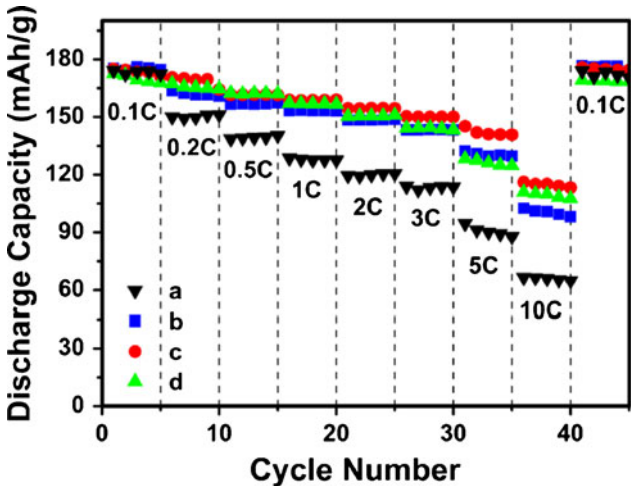

Fig. 6 Discharge capacity as a function of cycle number at different C rate. (*a*) Pristine $Li_4Ti_5O_{12}$, (*b*) $Li_4Ti_5O_{12}$/TiN(3 %), (*c*) $Li_4Ti_5O_{12}$/TiN (6 %), and (*d*) $Li_4Ti_5O_{12}$/TiN(12 %)

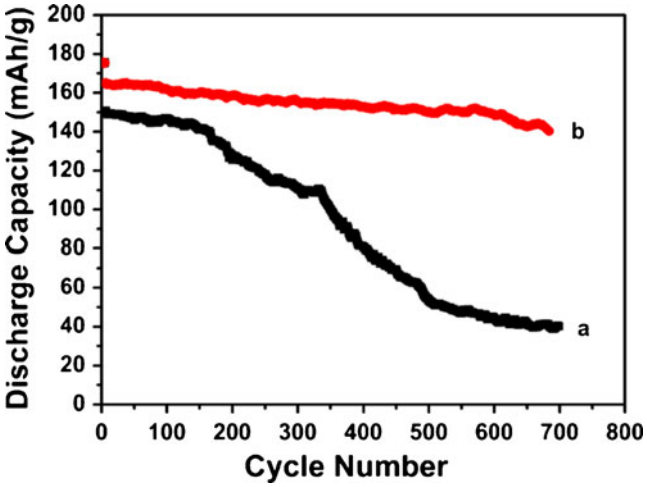

Fig. 7 Cycling performances of (*a*) pristine $Li_4Ti_5O_{12}$ and (*b*) $Li_4Ti_5O_{12}$/TiN(6 %)

nitridation has a large effect on the electrochemical behaviors of $Li_4Ti_5O_{12}$ at high rates. As demonstrated above, the TiN formed on the surface of the $Li_4Ti_5O_{12}$ particles can provide the contact sites to improve the electrical conductivity of the $Li_4Ti_5O_{12}$ particles. Compared to the $Li_4Ti_5O_{12}$/TiN(6 %) composite, the $Li_4Ti_5O_{12}$/TiN(3 %) composite may provide less conductive TiN sites and delivers less capacity. For the $Li_4Ti_5O_{12}$/TiN(12 %) composite, however, coverage of TiN should be much higher than that for the $Li_4Ti_5O_{12}$/TiN(6 %) composite. The fact that the $Li_4Ti_5O_{12}$/TiN(12 %) composite exhibited less capacity might be related to the fact that the electrochemical behaviors of the $Li_4Ti_5O_{12}$ particles depend on not only the electrical conductivity but also Li-ion transport of the material. Most likely, the surface TiN is less permeable for Li-ions; the excess TiN formed on the surface of the $Li_4Ti_5O_{12}$/TiN(12 %) composite may lead to less surface area of the $Li_4Ti_5O_{12}$ particles to be directly exposed to the electrolyte. In other words, the excess TiN on the surface may cause an additional barrier for Li-ion transport, although the conductivity of the oxide may be increased with increasing of the amount of TiN on the surface of the particles. Similar arguments have also been suggested in the case of the carbon-coated $Li_4Ti_5O_{12}$ particles [35]. It is important, therefore, that the extent of the surface nitridation should be optimized for the $Li_4Ti_5O_{12}$ particles in order to obtain a better performance of the material.

The cycling stability of the pristine $Li_4Ti_5O_{12}$ and $Li_4Ti_5O_{12}$/TiN(6 %) composite were compared at 3 C rate after the first five cycles at 0.2 C rate, the results are shown in Fig. 7. The capacities of the pristine $Li_4Ti_5O_{12}$ and $Li_4Ti_5O_{12}$/TiN(6 %) composite in the first cycle at 3 C rate were 150.9 and 165.1 mAh/g, respectively. After 100 cycles at 3 C rate, the loss of the capacities for 10 the pristine $Li_4Ti_5O_{12}$ and $Li_4Ti_5O_{12}$/TiN(6 %) composites were less than 2 %, indicating the capacities for both the samples were well retained. However, after 140 cycles, an accelerated decay in the capacity of the pristine $Li_4Ti_5O_{12}$ was observed, only 42.8 mAh/g of the capacity was obtained after 600 cycles. On the other hand, the capacity of the $Li_4Ti_5O_{12}$/TiN(6 %) composite was 148.3 mAh/g after 600 cycles, namely about 90 % of the initial capacity was still preserved, although a slow loss in capacity also existed for the $Li_4Ti_5O_{12}$/TiN(6 %) composite. These results demonstrate that the surface TiN can significantly improve the stability of the $Li_4Ti_5O_{12}$ particles during the charge–discharge cycling. In the literature, two main factors have been attributed to be responsible for the capacity loss of the $Li_4Ti_5O_{12}$ particles, including the catalytical decomposition of the electrolyte and mechanical failure of the surface layer of the $Li_4Ti_5O_{12}$ particles [36, 37]. Although the lithium insertion–extraction plateau of $Li_4Ti_5O_{12}$ is 1.5 V vs. Li^+/Li, which is higher than the reduction potential of most organic electrolytes, the reduction gases such as hydrocarbon and CO can still be generated during charge/discharge cycling of the batteries. The formation of the gas has been ascribed to the catalytical decomposition of the electrolytes on the surface active sites of the $Li_4Ti_5O_{12}$ particles [36]. In the case of the $Li_4Ti_5O_{12}$ (6 %) composite, however, the chemical inert TiN, dispersedly occupying the sites on the surface of the $Li_4Ti_5O_{12}$ particles, could prevent the electrolyte from catalytical degradation. On the other hand, as suggested by Borgols et al. [37], the larger Li-ion concentration in the surface layer could lead to a large distortion of the surface structure of the $Li_4Ti_5O_{12}$ particles. As a result, a mechanical failure of the thin surface layer structure could occur, leading to an irreversible capacity loss in the plateau region

of the $Li_4Ti_5O_{12}$ particles. In this case, the surface layer of the $Li_4Ti_5O_{12}$ particles is partially converted into relatively rigid TiN. As observed by the TEM image (Fig. 3c), the TiN zones are scattered over the surface of the $Li_4Ti_5O_{12}$ particles. The TiN zones with a crystal structure different from that of $Li_4Ti_5O_{12}$ thereby may relieve the stress from the distortion of the surface structure of the $Li_4Ti_5O_{12}$ particles and stabilize the $Li_4Ti_5O_{12}$ particles.

Conclusions

The surface of the $Li_4Ti_5O_{12}$ particles can be converted into the highly conductive and relatively stable TiN in a controllable manner by using urea as the nitrogen source. The electrochemical performance of the $Li_4Ti_5O_{12}$ particles is largely affected by the extent of the surface nitridation. The initial capacity and rate capability of the $Li_4Ti_5O_{12}$ particles could be greatly improved by optimizing the surface nitridation. The chemical inert TiN existing on the surface of the $Li_4Ti_5O_{12}$ particles may prevent the electrolyte from decomposition and stabilize the surface structure of the $Li_4Ti_5O_{12}$ particles, endowing the oxide with an excellent cycleability. The urea-nitridation strategy may also be a useful approach to improve the conductivity and stability of other metal oxides used as the electrode materials in lithium-ion batteries.

Acknowledgments Financial supports from the Nature Science Foundation of China (nos. 20873089, 20975073), Science and Technology Department of Jiangsu Province (nos. BY2011130), and State Key Laboratory of Lithium Ion Battery Materials of Jiangsu Province are gratefully acknowledged.

References

1. Etacheri V, Marom R, Elazari R, Salitra G, Aurbach D (2011) Energy Environ Sci 4:3243
2. Scrosati B, Garche J (2010) J Power Sources 195:2419
3. Yang Z, Zhang J, Kintner-Meyer MCW, Lu X, Choi D, Lemmon JP, Liu J (2011) Chem Rev 111:3577
4. Wu YP, Rahm E, Holze R (2003) J Power Sources 114:228
5. de las Casas C, Li W (2012) J Power Sources 208:74
6. Dai L, Chang DW, Baek J-B, Lu W (2012) Small 8:1130
7. Ohta N, Nagaoka K, Hoshi K, Bitoh S, Inagaki M (2009) J Power Sources 194:985
8. Jeong S-K, Seo H-Y, Kim D-H, Han H-K, Kim J-G, Lee YB, Iriyama Y, Abe T, Ogumi Z (2008) Electrochem Commun 10:635
9. Thackeray MM (1999) J Am Ceram Soc 82:3347
10. Yi T-F, Jiang L-J, Shu J, Yue C-B, Zhu R-S, Qiao H-B (2010) J Phys Chem Solid 71:1236
11. Sorensen EM, Barry SJ, Jung H-K, Rodinelli JR, Vaughey JT, Poeppelmeier KR (2006) Chem Mater 18:482
12. Kim H-K, Bak S-M, Kim K-B (2010) Electrochem Commun 12:1768
13. Jiang C, Ichihara M, Honma I, Zhou H (2007) Electrochim Acta 52:6470
14. Kim DH, Ahn YS, Kim J (2005) Electrochem Commun 7:1340
15. Abe Y, Matsui E, Senna M (2007) J Phys Chem Solid 68:681
16. Lee SC, Lee SM, Lee JW, Lee JB, Lee SM, Han SS, Lee HC, Kim HJ (2009) J Phys Chem 113:18420
17. Gao J, Ying J, Jiang C, Wan C (2009) Ionics 15:597
18. Capsoni D, Bini M, Massarotti V, Mustarelli P, Ferrari S, Chiodelli G, Mozzati MC, Galinetto P (2009) J Phys Chem C 113:19664
19. Tabuchi T, Yasuda H, Yamachi M (2006) J Power Sources 162:813
20. Yuan T, Yu X, Cai R, Zhou Y, Shao Z (2010) J Power Sources 195:4997
21. Wang GJ, Gao J, Fu LJ, Zhao NH, Wu YP, Takamura T (2007) J Power Sources 174:1109
22. Zhao L, Hu YS, Li H, Wang ZX, Chen LQ (2011) Adv Mater 23:1385
23. Liu H, Feng Y, Wang K, Xie J (2008) J Phys Chem Solid 69:2037
24. Snyder MQ, Trebukhova SA, Ravdel B, Wheeler MC, DiCarlo J, Tripp CP, DeSisto WJ (2007) J Power Sources 165:379
25. Park K-S, Benayad A, Kang D-J, Doo S-G (2008) J Am Chem Soc 130:14930
26. Giordano C, Erpen C, Yao WT, Milke B, Antonietti M (2009) Chem Mater 21:5136
27. Buha J, Djerdj I, Antonietti M, Niederberger M (2007) Chem Mater 19
28. Aldon L, Kubiak P, Womes M, Jumas JC, Olivier-Fourcade J, Tirado JL, Corredor JI, Vicente CP (2004) Chem Mater 16:5721
29. Scharner S, Schmid-Beurmann P, Weppner W (1999) J Electrochem Soc 146:857
30. Julien CM, Massot M, Zaghib K (2004) J Power Sources 136:72
31. Shu J, Shui M, Xu D, Gao S, Yi T, Wang D, Li X, Ren Y (2011) Ionics 17:503
32. Cheng YH, Tay BK, Lau SP, Kupfer H, Richter F (2002) J Appl Phys 92:1845
33. Guo X, Xie Y, Wang XJ, Lv SC, Hou T, Bai CN (2005) J Am Ceram Soc 88:249
34. Ge H, Li N, Li D, Dai CS, Wang DL (2009) J Phys Chem C 113:6324
35. Wang J, Liu X, Yang H, Shen X (2011) J Alloys Compd 509:712
36. He Y, Ning F, Li B, Song Q, Lv W, Du H, Zhai D, Su F, Yang Q, Kang F (2012) J Power Sources 202:253
37. Borghols WJH, Wagemaker M, Lafont U, Kelder EM, Mulder FM (2009) J Am Chem Soc 131:17786